Original

Li, Z.; Zhang, Y.; Esling, C.; Gan, W.; Zou, N.; Zhao, X.; Zuo, L.:

In-situ neutron diffraction study of martensitic variant redistribution in polycrystalline Ni-Mn-Ga alloy under cyclic thermo-mechanical treatment

In: Applied Physics Letters (2014) AIP

DOI: 10.1063/1.4890598

In-situ neutron diffraction study of martensitic variant redistribution in polycrystalline Ni-Mn-Ga alloy under cyclic thermo-mechanical treatment

Zongbin Li,[1] Yudong Zhang,[2,3,a)] Claude Esling,[2,3] Weimin Gan,[4] Naifu Zou,[1] Xiang Zhao,[1] and Liang Zuo[1,a)]

[1]*Key Laboratory for Anisotropy and Texture of Materials (Ministry of Education), Northeastern University, Shenyang 110819, China*
[2]*Laboratoire d'Étude des Microstructures et de Mécanique des Matériaux (LEM3), CNRS UMR 7239, Université de Lorraine, 57045 Metz, France*
[3]*Laboratory of Excellence on Design of Alloy Metals for low-mAss Structures (DAMAS), Université de Lorraine, 57045 Metz, France*
[4]*German Engineering Materials Science Centre (GEMS), Helmholtz-Zentrum Geesthacht (HZG) Outstation at FRM II, D-85748, Garching, Germany*

(Received 1 June 2014; accepted 7 July 2014; published online 17 July 2014)

The influences of uniaxial compressive stress on martensitic transformation were studied on a polycrystalline Ni-Mn-Ga bulk alloy prepared by directional solidification. Based upon the integrated *in-situ* neutron diffraction measurements, direct experimental evidence was obtained on the variant redistribution of seven-layered modulated (7M) martensite, triggered by external uniaxial compression during martensitic transformation. Large anisotropic lattice strain, induced by the cyclic thermo-mechanical treatment, has led to the microstructure modification by forming martensitic variants with a strong $\langle 0\ 1\ 0\rangle_{7M}$ preferential orientation along the loading axis. As a result, the saturation of magnetization became easier to be reached. © *2014 AIP Publishing LLC*. [http://dx.doi.org/10.1063/1.4890598]

Ni-Mn-Ga alloys, which combine the properties of ferromagnetism with those of a reversible martensitic transformation, are conceived as a novel class of multifunctional magnetic materials.[1–13] Under magnetic field, these alloys demonstrate not only giant magnetic shape memory effect but also significant magnetocaloric effect. For instance, large magnetic field-induced strains up to 12% can be achieved in single crystals,[10] originating from the magnetically driven reorientation of martensitic variants with strong magnetocrystalline anisotropy.[14] With the advantage of large output and fast dynamic response under magnetic field, such alloys have potential for various applications in actuators, sensors, and magnetic refrigeration systems.

So far, the superior magnetic shape memory performances have been revealed in Ni-Mn-Ga single crystals. Apparently, the high-cost fabrication of single crystals constitutes a severe obstacle for practical applications. In contrast, the preparation routes of polycrystalline alloys are much simpler and of lower cost. However, a more or less random distribution of crystallographic orientation presented in polycrystalline alloys would greatly weaken the orientation dependence of magnetocrystalline anisotropy, which severely impairs the magnetic shape memory properties. Thus, the microstructure texturing with proper processing routes should be seen as the best practice to resume the lost anisotropic features and to improve the functional behaviours of polycrystalline alloys.

In general, martensitic transformation is a deformation-dominant diffusionless structural change from high-symmetry austenite to low-symmetry martensite, which induces significant macroscopic shape change of the product phase with respect to its parent phase. This shape change is accommodated by forming groups of martensitic variants with certain morphologies and crystallographic orientations. As the shape change is anisotropic, imposition of a unidirectional constraint (tension or compression) could promote the formation of some favourable variants but prevent other unfavourable ones.[15] Therefore, strong preferential orientation of martensite may be achieved through the selective formation of favourable variants with the application of a bias field, as to realize the optimization of crystallographic and magnetocrystalline anisotropy. In the present study, the directional solidification method was used to prepare a polycrystalline Ni-Mn-Ga alloy, by which a strong $\langle 0\,0\,1\rangle_A$ crystallographic texture of austenite can be produced.[16] The thermo-mechanical treatment (TMT) incorporating three cycles of uniaxial compression was introduced during martensitic transformation to modify the variant distribution. With the integrated *in-situ* neutron diffraction, the martensitic transformation processes under uniaxial compression were traced and the direct evidence on the variant redistribution induced by TMT was captured.

A polycrystalline Ni-Mn-Ga alloy ingot with nominal composition of $Ni_{50}Mn_{30}Ga_{20}$ was prepared by directional solidification, followed by homogenization at 1173 K for 24 h. The actual composition was verified to be $Ni_{50.1}Mn_{28.8}Ga_{21.1}$ by energy dispersive spectroscopy attached to a scanning electron microscope. The room-temperature crystal structure was determined by powder X-ray diffraction (XRD). The martensitic transformation temperatures were measured by differential scanning calorimetry (DSC, TA Q100). The magnetic properties were measured with a vibrating sample magnetometer (VSM, Lakeshore 7407). The cylindrical-shaped samples with dimension of

a)Authors to whom correspondence should be addressed. Electronic addresses: lzuo@mail.neu.edu.cn and yudong.zhang@univ-lorraine.fr.

ϕ5 mm × 10 mm were cut from the ingot for the cyclic TMT and neutron diffraction.

The *in-situ* TMT and neutron diffraction experiments were performed using the materials science diffractometer STRESS-SPEC operated by FRM II and HZG at the Heinz Maier-Leibnitz Zentrum (MLZ), Garching, Germany, with a monochromatic wavelength of 2.1 Å.[17] The uniaxial compressive load was applied by a rotatable multifunctional (tension/compression/torsion) load frame installed at STRESS-SPEC,[18] with the "constant load" mode to ensure a fixed load. For the *in-situ* measurements on the cyclic TMT, one cylindrical-shaped sample was first heated from room temperature to 393 K to reach the fully austenite state, where a uniaxial compressive load of −10 MPa was applied on cooling along the solidification direction (SD). Then, the sample was cooled to room temperature at a cooling rate of 2 K/min under the constant load, during which the neutron diffraction images were recorded at a time interval of 60 s by a two-dimensional (2D) detector at $2\theta = 43.5°$. These two steps were taken as to constitute Cycle 1 of the TMT. For Cycles 2 and 3, the experimental conditions were the same as those of Cycle 1, except that the constant compressive load was set to be −25 MPa and −50 MPa, respectively. The macroscopic strain changes of the tested sample in each cycle were measured by the clip-on extensometers in the load frame. Besides, the global crystallographic textures of the initial sample (without TMT) and the treated sample (with three TMT cycles) were examined *ex-situ*. The incoming beam sizes for the *in-situ* neutron diffraction and the *ex-situ* pole figure measurements were 5 mm × 5 mm and ϕ15 mm, respectively. The SteCa software was used to extract diffraction patterns and pole figures from the recorded 2D diffraction images.[19]

For the present directionally solidified and homogenized alloy, the start and finish temperatures of the forward and backward martensitic transformations, determined from the DSC curves, are, respectively, 347.8 K (M_s), 331.3 K (M_f), 336.8 K (A_s), and 352.2 K (A_f). Powder XRD analyses show that the alloy consists of seven-layered modulated (7M) martensite at room temperature, having a monoclinic incommensurate superstructure with lattice parameters $a_{7M} = 4.2651$ Å, $b_{7M} = 5.5114$ Å, $c_{7M} = 42.365$ Å, and $\beta = 93.27°$. Under this superstructure frame, the easy magnetization axis of the 7M martensite corresponds to the b axis of the superstructure, i.e., $[0\ 1\ 0]_{7M}$.[20]

Fig. 1 shows the room-temperature microstructure of the studied alloy at the initial state. It can be seen that original austenite grains are columnar-shaped along the SD, with an average grain size of ~500 μm. For cubic structured metals, the $\langle 0\,0\,1\rangle_A$ crystallographic directions are the principal crystal growth directions during solidification.[16] Thus, for the present alloy, the columnar-shaped austenite grains should have a strong $\langle 0\,0\,1\rangle_A$ preferred orientation parallel to the SD.

Fig. 2(a) shows the neutron diffraction patterns of the initial cylindrical-shaped sample. At room temperature (~303 K), four diffraction peaks of 7M martensite, i.e. $(\bar{1}\,0\,10)_{7M}$, $(1\,0\,10)_{7M}$, $(0\,2\,0)_{7M}$, and $(1\,0\,13)_{7M}$, were detected in the 2θ range of ~36°–52° (Fig. 2(a)-lower), where the $(1\,0\,10)_{7M}$ diffraction possesses the strongest intensity. Within the measured 2θ range, only the $(2\,0\,0)_A$ diffraction can be observed in the austenite temperature region (Fig. 2(a)-upper). Figs. 2(b)–2(d) display the serial patterns measured on cooling across the martensitic transformation under the compressive load of −10 MPa (Cycle 1), −25 MPa (Cycle 2), and −50 MPa (Cycle 3), respectively. It is seen from Fig. 2(b) that under −10 MPa, the martensitic transformation started at around 348.7 K and finished at around 335.9 K. Compared with the initial sample, the compressive load of −10 MPa has led to a certain increase in M_s (~0.9 K). Moreover, the strongest diffraction peak of 7M martensite was changed to the $(0\ 2\ 0)_{7M}$, suggesting a redistribution of martensitic variants induced by the applied load during the martensitic transformation. For Cycle 2 under

FIG. 1. Microstructure of directionally solidified and homogenized alloy at room temperature, showing the columnar-shaped morphology of original austenite grains.

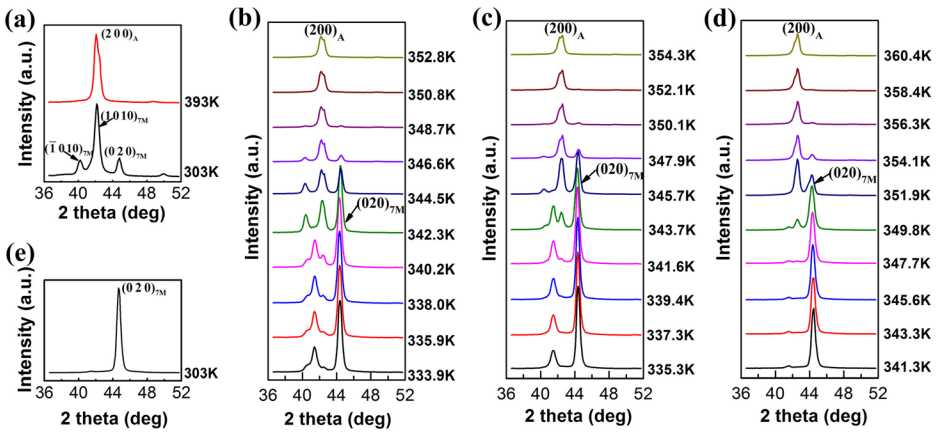

FIG. 2. (a) Neutron diffraction pattern measured on initial sample at ~393 K and ~303 K. (b)–(d) Neutron diffraction patterns measured on TMT sample during cooling under compressive load of −10 MPa (Cycle 1), −25 MPa (Cycle 2), and −50 MPa (Cycle 3). (e) Neutron diffraction pattern measured on TMT sample at ~303 K without compressive load after three TMT cycles.

−25 MPa (Fig. 2(c)), the martensitic transformation started at around 350.1 K and finished at around 339.4 K, being slightly higher than the corresponding temperatures of Cycle 1. Meanwhile, the $(0\ 2\ 0)_{7M}$ diffraction intensity of 7M martensite was increased with respect to Cycle 1. As for Cycle 3 under −50 MPa (Fig. 2(d)), the martensitic transformation further shifted to a higher temperature region ($M_s = 356.3$ K and $M_f = 345.6$ K). After the completion of three TMT cycles, there remained at room temperature almost only the $(0\ 2\ 0)_{7M}$ diffraction in the measured 2θ range (Fig. 2(e)). Apparently, the uniaxial compression has exerted significant influence on the variant distribution, creating a strong preferential orientation of the $(0\ 2\ 0)_{7M}$ plane.

Fig. 3 presents the macroscopic shape changes of the tested sample, recorded *in-situ* in each cycle. It is seen that the compressive load applied during martensitic transformation resulted in considerable macroscopic strain. With an increasing load, the deformation amount increased gradually, i.e., −2.1%, −2.8%, and −3.3% for Cycle 1, Cycle 2, and Cycle 3, respectively. Such a trend may also indicate the increase in the degree of preferred variant orientation. Here, the gradual strain changes before and after the martensitic transformation could be due to the shrinkage on cooling, which were also observed by other authors.[21,22]

According to the *in-situ* neutron diffraction measurements, the uniaxial compression can significantly influence the martensitic transformation thermodynamics, resulting in increased transformation temperatures. The increases of M_s under −10 MPa, −25 MPa, and −50 MPa were ∼0.9 K, ∼2.3 K, and ∼8.5 K, respectively. The shifts of transformation temperature under uniaxial load σ in the present work can well be described by the Clausius-Clapeyron equation: $d\sigma/dT = -\Delta S \cdot \rho/\varepsilon$, where ΔS and ε stand, respectively, for the entropy change and transformation strain, and ρ is the mass density. Here, ΔS was determined from the DSC measurements to be ∼21.7 $Jkg^{-1}K^{-1}$, and ρ was taken as ∼7.964 $g \cdot cm^{-3}$.[23] By inputting the corresponding values to the Clausius-Clapeyron equation, it derives that the uniaxial load of −10 MPa, −25 MPa, and −50 MPa can result in the respective increase of 1.2 K, 4.1 K, and 9.5 K in M_s, being rather close to the observed transformation temperature shifts.

Fig. 4 shows the backscattered electron (BSE) images of the initial sample and the TMT sample. Initially, the 7M martensite plates exhibit typical self-accommodated

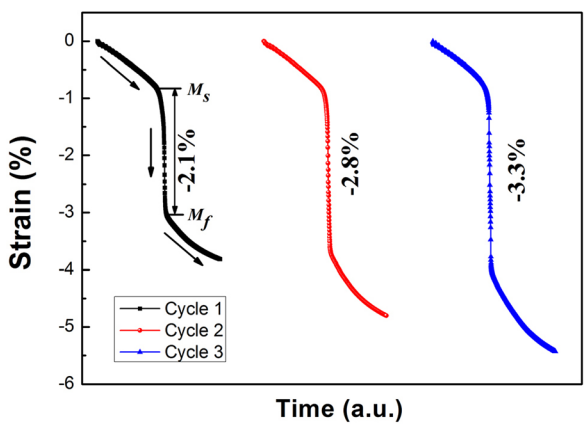

FIG. 3. Macroscopic strain curves of tested sample under three TMT cycles.

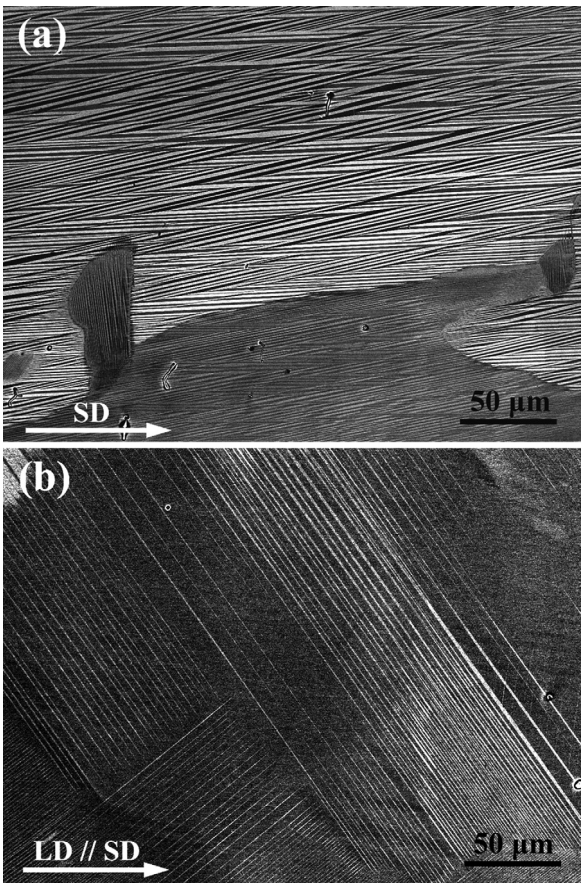

FIG. 4. (a) BSE image of 7M martensite without TMT. (b) BSE image of 7M martensite after three TMT cycles.

microstructure (Fig. 4(a)). There appear a certain bending in some plates and most of them tend to be parallel to the SD. Besides, the neighbouring plates are very close in plate thickness. After the cyclic treatment (Fig. 4(b)), the 7M plates are straighter and tend to be oriented with an angle of ∼45° to the loading direction (LD). It is noted that the thickness ratio of neighbouring plates has changed greatly, i.e., one plate is much thicker than the other. Especially, the thinner plates almost disappeared in some local regions. This simpler variant configuration should be originated from the accommodation of the external compression by suppressing certain unfavourable variants. Moreover, such kind of variant arrangement should be also advantageous for the variant interface movement. As demonstrated by Straka *et al.*,[24] a mixture of differently oriented variants exhibited a relatively large twinning stress, whereas the single-variant or two-variant microstructure could result in a reduced twinning stress, which is much easier for variant reorientation.

To have further insight into the variant redistribution induced by cyclic TMT, the complete pole figures were constructed using the neutron diffraction data. Since the easy magnetization axis is an important parameter for the magnetocrystalline anisotropy in Ni-Mn-Ga alloys, we shall focus on the orientation distribution of the easy magnetization axis of 7M martensite (i.e., $\langle 0\,1\,0\rangle_{7M}$). Fig. 5 displays the $(0\,2\,0)_{7M}$ complete pole figures of the sample before and after the cyclic TMT. In the initial sate (Fig. 5(a)), the $\langle 0\,1\,0\rangle_{7M}$ directions tend to be perpendicular or parallel to the SD. After the three cycles of treatment (Fig. 5(b)), the

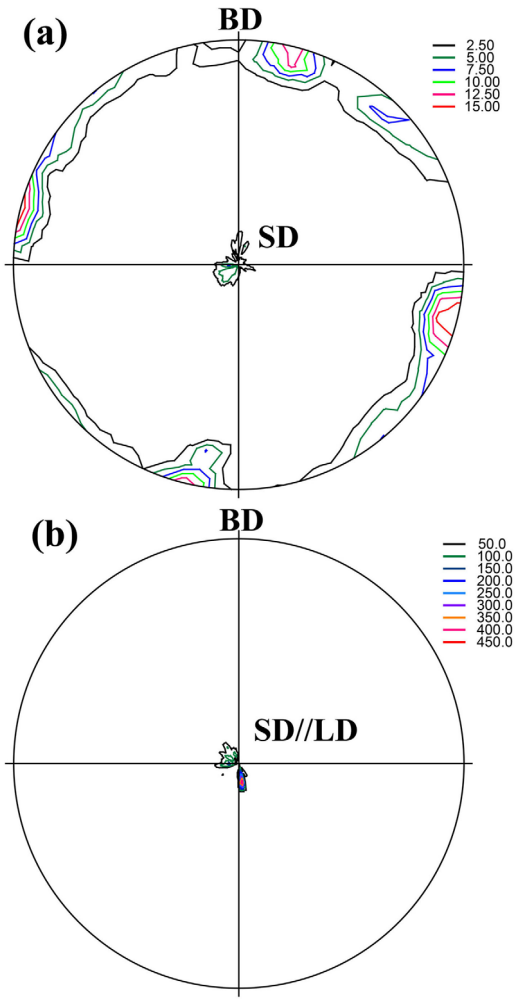

FIG. 5. (a) $(0\ 2\ 0)_{7M}$ pole figure of initial sample. (b) $(0\ 2\ 0)_{7M}$ pole figure of TMT sample with three cycles of treatment. Note: BD - incoming beam direction; SD - solidification direction; and LD – loading direction.

$\langle 0\ 1\ 0\rangle_{7M}$ directions become almost parallel to the LD (//SD). Notably, a strong $\langle 0\ 1\ 0\rangle_{7M}$ preferential orientation along the LD was induced by the external compression during the martensitic transformation.

Fig. 6 shows the magnetization curves of the samples without and with the cyclic TMT, measured along the SD.

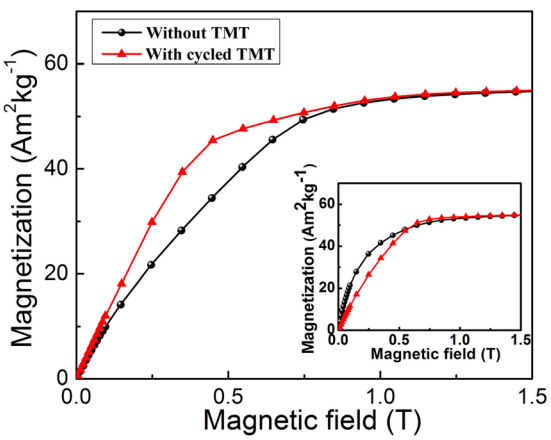

FIG. 6. Room-temperature magnetization curves measured on samples without and with TMT along SD (//LD). Inset: measured perpendicular to the SD (//LD).

Evidently, the magnetization of the sample after the cyclic TMT is much easier to reach the saturation, due to the presence of a strong $\langle 0\ 1\ 0\rangle_{7M}$ preferential orientation along the LD. The inset of Fig. 6 displays the magnetization curves of the samples measured perpendicular to the SD (//LD). In this situation, the TMT sample is more difficult to reach the saturation magnetization, as compared to the initial sample.

For directionally solidified Ni-Mn-Ga alloys, austenite grains form preferentially in columnar shape with their $\langle 1\ 0\ 0\rangle_A$ directions along the SD.[16] This orientation particularity can be indirectly deduced from the $(0\ 2\ 0)_{7M}$ pole figure of the initial sample without TMT (Fig. 5(a)), where the $\langle 0\ 1\ 0\rangle_{7M}$ directions tend to be perpendicular or parallel to the SD. With the Pitsch orientation relationship valid for the austenite to 7M martensite transformation,[25] it can be predicted that parent austenite grains possess a strong $\langle 1\ 0\ 0\rangle_A$ preferential orientation parallel to the SD. As the $\langle 0\ 1\ 0\rangle_{7M}$ of 7M martensite is inherited from the $\langle 1\ 0\ 0\rangle_A$ of austenite with a reduction of the atomic spacing, the formation of 7M martensite plates having the $\langle 0\ 1\ 0\rangle_{7M}$//SD becomes more favourable under the uniaxial compression.

Further analyses demonstrate that the compressive load induces certain lattice strain in austenite. The lattice strain ε_{hkl} in the direction normal to a $(h\,k\,l)$ lattice plane can be evaluated from measured interplanar spacing (d_{hkl}) using the equation: $\varepsilon_{hkl} = (d_{hkl} - d_{0,hkl})/d_{0,hkl}$,[26] where $d_{0,hkl}$ is the stress-free reference interplanar spacing. Prior to the martensitic transformation, the lattice strains of the $(2\ 0\ 0)_A$ plane under the compressive load are determined to be -0.007 (-10 MPa), -0.0096 (-25 MPa), and -0.0105 (-50 MPa), respectively. These lattice strains would initiate the martensitic transformation and break the self-accommodation state of martensitic variants. To accommodate these lattice strains of austenite, variants with the $\langle 0\ 1\ 0\rangle_{7M}$//LD form preferentially, leading to the macroscopic strain and the formation of a strong $\langle 0\ 1\ 0\rangle_{7M}$ preferred orientation along the LD.

In summary, the influences of uniaxial compression on martensitic transformation in a directionally solidified Ni-Mn-Ga polycrystalline alloy were studied by neutron diffraction. The cyclic TMT resulted in large unidirectional lattice strains for the martensitic transformation and hence great change in the martensite microstructure. The 7M martensite plates formed with a strong $\langle 0\ 1\ 0\rangle_{7M}$ preferential orientation along the loading axis, along which the saturation of magnetization was more easily reached. The present investigations may provide the fundamental information on variant selection subject to external stress field and the necessary guidelines for microstructure optimization of polycrystalline alloys through external field training.

The authors gratefully acknowledge the help from Dr. M. Hofmann and Dr. P. Juergen at FRM II during the neutron experiment, and the support from the European Union's 7th Framework Programme for research, technological development and demonstration under the NMI3-II Grant No. 283883. Financial supports from the 863 Program of China (Grant No. 2014AAQ00297), the 111 Program of China (Grant No. B07015), the Program for Liaoning Innovative Research Team in University (Grant No. LT2013007), the PhD Start-up Found of Liaoning

Province (Grant No. 20141001), the Fundamental Research Funds for the Central Universities of China (Grant No. N130110001), and the French State through the Investment in the Future Program operated by the National Research Agency and referenced by ANR-11-LABX-0008-01 (LabEx DAMAS), are highly appreciated.

[1]D. C. Dunand and P. Müllner, Adv. Mater. **23**, 216 (2011).
[2]K. Ullakko, J. K. Huang, C. Kantner, R. C. O'Handley, and V. V. Kokorin, Appl. Phys. Lett. **69**, 1966 (1996).
[3]P. Müllner, V. A. Chernenko, and G. Kostorz, J. Appl. Phys. **95**, 1531 (2004).
[4]U. Gaitzsch, M. Pötschke, S. Roth, B. Rellinghaus, and L. Schultz, Acta Mater. **57**, 365 (2009).
[5]H. E. Karaca, I. Karaman, B. Basaran, D. C. Lagoudas, Y. I. Chumlyakov, and H. J. Maier, Acta Mater. **55**, 4253 (2007).
[6]M. Chmielus, X. X. Zhang, C. Witherspoon, D. C. Dunand, and P. Müllner, Nat. Mater. **8**, 863 (2009).
[7]A. Planes, L. Mañosa, and M. Acet, J. Phys.: Condens. Matter **21**, 233201 (2009).
[8]S. J. Murray, M. Marioni, S. M. Allen, R. C. O'Handley, and T. A. Lograsso, Appl. Phys. Lett. **77**, 886 (2000).
[9]A. Sozinov, A. A. Likhachev, N. Lanska, and K. Ullakko, Appl. Phys. Lett. **80**, 1746 (2002).
[10]A. Sozinov, N. Lanska, A. Soroka, and W. Zou, Appl. Phys. Lett. **102**, 021902 (2013).
[11]Z. B. Li, J. L. Sánchez Llamazares, C. F. Sánchez-Valdés, Y. D. Zhang, C. Esling, X. Zhao, and L. Zuo, Appl. Phys. Lett. **100**, 174102 (2012).
[12]M. Pasquale, C. P. Sasso, L. H. Lewis, L. Giudici, T. Lograsso, and D. Schlagel, Phys. Rev. B **72**, 094435 (2005).
[13]Z. B. Li, Y. D. Zhang, C. F. Sánchez-Valdés, J. L. Sánchez Llamazares, C. Esling, X. Zhao, and L. Zuo, Appl. Phys. Lett. **104**, 044101 (2014).
[14]R. C. O'Handley, S. J. Murray, M. Marioni, H. Nembach, and S. M. Allen, J. Appl. Phys. **87**, 4712 (2000).
[15]Y. D. Wang, D. W. Brown, H. Choo, P. K. Liaw, D. Y. Cong, M. L. Benson, and L. Zuo, Phys. Rev. B **75**, 174404 (2007).
[16]C. Jiang, J. Liu, J. Wang, L. Xu, and H. Xu, Acta Mater. **53**, 1111 (2005).
[17]H. G. Brokmeier, W. M. Gan, C. Randau, M. Voeller, J. Rebelo-Kornmeier, and M. Hofmann, Nucl. Instrum. Methods Phys. Res., Sect. A **642**, 87 (2011).
[18]M. Hoelzel, W. M. Gan, M. Hofmann, C. Randau, G. Seidl, Ph. Jüttner, and W. W. Schmahl, Nucl. Instrum. Methods Phys. Res., Sect. A **711**, 101 (2013).
[19]C. Randau, U. Garbe, and H. G. Brokmeier, J. Appl. Crystallogr. **44**, 641 (2011).
[20]Z. B. Li, Y. D. Zhang, C. Esling, X. Zhao, Y. D. Wang, and L. Zuo, J. Appl. Crystallogr. **43**, 617 (2010).
[21]O. Heczko and L. Straka, Mater. Sci. Eng., A **378**, 394 (2004).
[22]A. Rudajevová, M. Frost, and A. Jäger, Mater. Sci. Technol. **23**, 542 (2007).
[23]L. Righi, F. Albertini, E. Villa, A. Paoluzi, G. Calestani, V. Chernenko, S. Besseghini, C. Ritter, and F. Passaretti, Acta Mater. **56**, 4529 (2008).
[24]L. Straka, O. Heczko, and H. Hänninen, Acta Mater. **56**, 5492 (2008).
[25]Z. B. Li, Y. D. Zhang, C. Esling, X. Zhao, and L. Zuo, Acta Mater. **59**, 2762 (2011).
[26]R. L. Peng, Y. D. Wang, Z. H. Nie, E. C. Oliver, S. Johansson, Y. D. Liu, Y. Ren, J. D. Jorgensen, and J. Fieramosca, J. Phys.: Condens. Matter **20**, 104256 (2008).